Neuroprotective Effects of Transcription Factor Brn3b in an Ocular Hypertension Rat Model of Glaucoma

Dorota L. Stankowska,[1] Alena Z. Minton,[1] Margaret A. Rutledge,[2] Brett H. Mueller II,[2] Nitasha R. Phatak,[1] Shaoqing He,[1] Hai-Ying Ma,[2] Michael J. Forster,[2] Thomas Yorio,[2] and Raghu R. Krishnamoorthy[1]

[1]University of North Texas Health Science Center, Department of Cell Biology and Immunology, North Texas Eye Research Institute, Fort Worth, Texas, United States
[2]University of North Texas Health Science Center, Department of Pharmacology & Neuroscience, Fort Worth, Texas, United States

Correspondence: Dorota L. Stankowska, Department of Cell Biology and Immunology, North Texas Eye Research Institute, UNT Health Science Center, 3500 Camp Bowie Boulevard, Fort Worth, TX 76107, USA;
dorota.stankowska@unthsc.edu.

Submitted: June 11, 2014
Accepted: December 18, 2014

Citation: Stankowska DL, Minton AZ, Rutledge MA, et al. Neuroprotective effects of transcription factor Brn3b in an ocular hypertension rat model of glaucoma. *Invest Ophthalmol Vis Sci*. 2015;56:893–907. DOI:10.1167/iovs.14-15008

Purpose. Glaucoma is an optic neuropathy commonly associated with elevated intraocular pressure (IOP), leading to optic nerve head (ONH) cupping, axon loss, and apoptosis of retinal ganglion cells (RGCs), which could ultimately result in blindness. Brn3b is a class-4 POU domain transcription factor that plays a key role in RGC development, axon outgrowth, and pathfinding. Previous studies suggest that a decrease in Brn3b levels occurs in animal models of glaucoma. The goal of this study was to determine if adeno-associated virus (AAV)-directed overexpression of the Brn3b protein could have neuroprotective effects following elevated IOP-mediated neurodegeneration.

Methods. Intraocular pressure was elevated in one eye of Brown Norway rats (*Rattus norvegicus*), following which the IOP-elevated eyes were intravitreally injected with AAV constructs encoding either the GFP (rAAV-CMV-GFP and rAAV-hsyn-GFP) or Brn3b (rAAV-CMV-Brn3b and rAAV-hsyn-Brn3b). Retina sections through the ONH were stained for synaptic plasticity markers and neuroprotection was assessed by RGC counts and visual acuity tests.

Results. Adeno-associated virus–mediated expression of the Brn3b protein in IOP-elevated rat eyes promoted an upregulation of growth associated protein-43 (GAP-43), actin binding LIM protein (abLIM) and acetylated α-tubulin (ac-Tuba) both posterior to the ONH and in RGCs. The RGC survival as well as axon integrity score were significantly improved in IOP-elevated rAAV-hsyn-Brn3b–injected rats compared with those of the IOP-elevated rAAV-hsyn-GFP–injected rats. Additionally, intravitreal rAAV-hsyn-Brn3b administration significantly restored the visual optomotor response in IOP-elevated rat eyes.

Conclusions. Adeno-associated virus–mediated Brn3b protein expression may be a suitable approach for promoting neuroprotection in animal models of glaucoma.

Keywords: Brn3b, glaucoma, Morrison's model, neuroprotection, gene therapy

Glaucoma is an optic neuropathy characterized by optic nerve degeneration, apoptosis of retinal ganglion cells (RGCs), and visual field loss.[1] A major risk factor for the disease is an elevation of IOP. Most current treatments for glaucoma are therefore aimed at lowering IOP, thereby limiting the primary insult that produces axonal degeneration of the optic nerve and loss of RGCs. However, despite lowering IOP, some neurodegenerative effects persistently occur in the optic nerve head and retina, albeit at a slower pace. Therefore, it would be beneficial to develop strategies to promote neuroprotection of the optic nerve and RGCs as an adjunct therapy for glaucoma.

The brain-specific homeobox/POU domain protein (Brn) family of class-4 POU domain transcription factors including Brn3a, Brn3b, and Brn3c has been shown to play an important role in the development of restricted neuronal populations in the central nervous system (CNS). In the retina, Brn3b is expressed by retinal ganglion precursor neurons as well as mature RGCs.[2–4] Brn3b has been shown to be a key regulator of axon outgrowth and pathfinding in RGCs and contributes to their proper polarization.[5–7] The predominant phenotype in Brn3b-deficient mice, but not Brn3a- or Brn3c-deficient mice, was loss of most ganglion cells, with approximately 70% of RGCs undergoing apoptosis between E15.5 and birth.[2,8] Lack of Brn3b expression also caused a decline in the number of optic nerve fibers and thinning of the mouse optic nerve.[2] While a lack of Brn3b resulted in a developmental loss of RGCs due to the inability to develop axons, it is unclear if upregulating Brn3b expression could promote neuroprotection of RGCs and optic nerve axons following damage to the optic nerve. Here, we used an IOP-elevated rat model of optic nerve damage to assess the ability of adeno-associated virus serotype 2 (AAV-2) overexpressing transcription factor Brn3b to promote neuroprotection of RGCs and maintenance of axonal integrity. Our data strongly suggest that AAV-mediated Brn3b protein expression may be a suitable agent to promote neuroprotection of RGCs and their axons during ocular hypertension in rodents.

Materials and Methods

Plasmid Construction and Recombinant AAV-2 Production

Recombinant AAV vectors were prepared using plasmids pAAV-IRES-hrGFP (hrGFP is a humanized recombinant GFP), pAAV-RC, and pHelper (AAV Helper-Free System; Stratagene, La Jolla, CA, USA) as described by the manufacturer. In this system, AAV2 rep and cap genes were provided by pAAV-RC plasmid. pAAV-Brn3b vector encoding transcription factor Brn3b was constructed by insertion of mouse Brn3b cDNA clone (OriGene, Rockville, MD, USA) digested with *EcoRI* and *XhoI* into pAAV-IRES-hrGFP (Stratagene) abbreviated as pAAV-CMV-Brn3b. After DNA sequence validation, the pAAV-Brn3b plasmid was used for AAV-2 virus production (rAAV-CMV-Brn3b). A pAAV-IRES-hrGFP control plasmid (Stratagene) was used for production of control virus and was abbreviated further as rAAV-CMV-GFP. Gene expression in both vectors was driven by cytomegalovirus (CMV) promoter. From the recombinant vector, Brn3b protein was expressed as fused with Flag-tag. Viruses were prepared according to manufacturer's instruction (AAV Helper-Free System; Stratagene) and purified by column chromatography using a commercially available kit (ViraBind AAV Purification Kit; Cell Biolabs, Inc., San Diego, CA, USA). Viral titers were determined using a Quick Titer AAV Kit (Cell Biolabs, Inc.).

To improve the specificity and reduce off target effects of the AAV-2 virus, in further studies we decided to use the viral constructs driven by neuronal specific human synapsin promoter. The control virus AAV2.hSyn.eGFP.WPRE.bGH was purchased from the Penn vector core facility (Philadelphia, PA, USA) and further abbreviated in the manuscript as rAAV-hsyn-GFP. The pAAV-hSyn.Brn3b-DDK.WPRE.bGH plasmid was prepared by insertion of mouse Brn3b cDNA clone (OriGene, Rockville, MD, USA) containing DDK tag with introduced HindIII restriction digestion site by PCR method into pAAV.hSyn.eGFP.WPRE.bGH in the place of eGFP protein using EcoRI and HindIII restriction enzymes. The custom-made plasmid sequence was confirmed by DNA sequencing and sent to Penn vector core for AAV-2 virus production. The custom-made virus AAV2.hSyn.Brn3b-DDK.WPRE.bGH was abbreviated in the current study as rAAV-hsyn-Brn3b.

Animals

All animal-related procedures were approved by the Institutional Animal Care and Use Committee (IACUC) at the UNT Health Science Center and were in compliance with the ARVO Statement for the Use of Animals in Ophthalmic and Vision Research. Male retired breeder Brown Norway rats (*Rattus norvegicus*; Charles River Laboratories, Wilmington, MA, USA) in the age group of 8 to 12 months were used in this study. Animals were maintained under dim light (90 lux) with a standard rodent diet. For retinal explants, eyes from adult female Sprague Dawley rats were used.

Retrograde Labeling of RGCs With Fluorogold

Retrograde labeling of RGCs was carried out in Brown Norway rats as described earlier.[9] The animals were anesthetized and double injections of 3 μL of 2% Fluorogold (Fluorochrome, LLC, Denver, CO, USA), were carried out using two sets of stereotaxic coordinates: (1) anterior posterior (AP) = 5.8, ML = +1.3, DV = 3.5, and (2) AP = 5.8, ML = −1.3, DV = 3.5 from the bregma.

Experimental Glaucoma Development – Morrison's Model

To elevate IOP approximately 50 μL 1.8 M NaCl was injected into episcleral veins of the left eye of rats with a force sufficient to blanch the aqueous plexus. This procedure produces scarring of the trabecular meshwork with a resultant rise in IOP and damage to the optic nerve.[10]

Elevation of IOP and IOP Measurements

Intraocular pressure was measured with a TonoLab tonometer (Icare Finland Oy, Espoo, Finland) in conscious animals after minimal sedation with intraperitoneal administration of 50 μL acepromazine and presented as mean ± SEM. To assess total IOP exposure, we calculated the mm Hg-days by determining the difference of area under the curve (AUC) between IOP-elevated eye and contralateral control eye (mm Hg-days = AUC of the IOP-elevated eye − AUC of the control eye).

Intravitreal Injections of AAV-2 Constructs

Intravitreal injections were carried out using an ultrafine 30.5-G disposable needle connected to a 50-μL Hamilton syringe (Hamilton Company, Reno, NV, USA) as described by Zhou and colleagues[11] in anesthetized rats. Four microliters containing 1×10^9 units of AAV virus were injected (with continuous observation of the needle) in the center of the vitreous cavity to avoid lens injury. Transduction of AAV viruses did not cause any inflammatory or damaging effect to the optic nerve or the retina. Experiments were performed five times in Brown Norway rat groups (total $n = 29$).

Anterograde Labeling of Axons Using Cholera Toxin (CT-B)

Two days prior to euthanization, rats were anesthetized and injected intravitreally with 4 μL 0.1% cholera toxin B subunit (CT-B) conjugated with Alexa Fluor 555 (Fig. 2A; Invitrogen, Life Technologies, Grand Island, NY, USA). Following euthanization and enucleation, eye cups and optic nerves were isolated and cryosectioned. Experiments employing CT-B injections were performed using five Brown Norway rats per experimental group.

Visual Threshold Measurements

An optomotor response test was carried out to assess visual function, using OptoMotry testing apparatus (OptoMotry, CerebralMechanics, AL, Canada), both prior to any manipulation and after administration of either rAAV-hsyn-GFP ($n = 7$) or rAAV-hsyn-Brn3b ($n = 7$) viral vectors in IOP-elevated rat eyes (Scheme; Fig. 2A). This behavioral test takes advantage of the optomotor response in which an animal reflexively follows a moving visual stimulus with its eyes, thereby compensating for rotation of the visual field. The walls of the test apparatus consisted of four computer monitors facing inward, with an elevated platform in the center of the chamber. An unrestrained rat was placed on the platform. Vertical sine-wave gratings (black vertical lines) were projected onto the white walls, and when the gratings were rotated, the rat responded by tracking the moving grating with its head and eyes. The spatial frequency of the gratings was gradually increased (i.e., the vertical lines are brought closer together) until the rat no longer detected the grating as distinct from the background. At this point, the rat ceased to respond to the rotating stimulus, and visual acuity was determined by the maximum spatial frequency (cycles/degrees) to which the animal has respond-

Investigative Ophthalmology & Visual Science

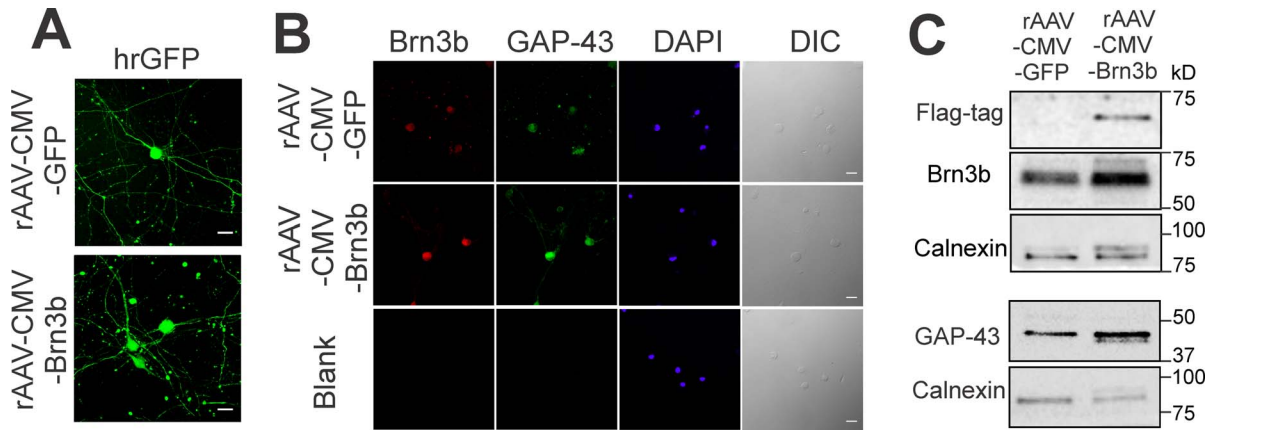

Figure 1. Adeno-associated virus–mediated increased level of Brn3b produced an increase in GAP43 in cultured rat primary RGCs. (**A**) Confocal images of primary RGCs transduced with 1×10^7 units of either rAAV-CMV-GFP or rAAV-CMV-Brn3b viruses. Expression of hrGFP in primary RGCs, 2 weeks after transduction of rAAV-CMV-GFP or rAAV-CMV-Brn3b. *Scale bar*: 20 μm. (**B**) Primary RGCs transduced with 1×10^7 units of rAAV-CMV-Brn3b showed an increase in immunostaining for Brn3b (*pseudo-red*) and GAP-43 (*pseudo-green*) compared with RGCs treated with rAAV-CMV-GFP virus. Cells were counterstained with DAPI to indicate cell nuclei. The *lower panel* (Blank) indicates immunostaining with the secondary antibodies conjugated with Alexa 555 (*pseudo-colored green*) or 647 (*pseudo-colored red*) dye alone (to determine nonspecific staining). *Scale bar*: 20 μm. (**C**) Immunoblot analysis of Flag-tag, Brn3b, and GAP-43 protein levels in primary RGCs transduced either with rAAV-CMV-GFP or rAAV-CMV-Brn3b vectors. The blots were probed for calnexin as a loading control.

ed. Acuity of both the left and right eye was assessed independently, by rotating stimuli in either a clockwise direction (thereby effectively testing the left eye) or a counterclockwise direction (thus, testing the right eye). The experimenter performing the behavioral tests was masked to the identity and treatment group of the rats. *T*-test was used to estimate significant difference between contralateral and operated eyes and paired *t*-tests were used to estimate the statistical difference in visual acuity before and after IOP elevation and following AAV treatment ($n = 7$/experimental group).

Quantification of RGC Survival

Fluorogold-labeled RGC cells were manually counted by a masked observer. Each retina was divided into four quadrants: superior, inferior, nasal, and temporal. Four pictures were taken at ×20 magnification in each retinal quadrant. Briefly, the number of RGCs was counted in four areas per retinal quadrant at two different eccentricities (E1 and E2) located at 2/6 and 4/6 of the radius of the retina from the optic nerve head respectively. The ratio of number of Fluorogold-labeled cells from IOP-elevated eye (injected with either rAAV-hsyn-GFP or rAAV-hsyn-Brn3b, $n = 4$/group) to contralateral eye was calculated and plotted as mean ± SEM. Statistical significance was estimated using *t*-test.

Paraphenylenediamine (PPD) Staining

Intraocular pressure elevation was carried out in Brown Norway rats and the animals were maintained for 4 weeks after IOP elevation, following which they were injected either with rAAV-hsyn-GFP or rAAV-hsyn-Brn3b viruses and killed after an additional 4 weeks. The eyes were enucleated and optic nerves were excised 1-mm posterior to the globe. The optic nerves were fixed with 2% paraformaldehyde, 2.5% glutaraldehyde in 0.1 M sodium cacodylate buffer for 3 hours at room temperature. After osmification and embedding in epon, optic nerve cross sections were obtained and stained with 1% PPD for 20 minutes at room temperature according to protocol of Hollander and Vaaland.[12] Images were taken in a Zeiss LSM 510 META confocal microscope (Carl Zeiss Microscopy GmbH, Jena, Germany). The images were graded in a masked manner by individuals giving a score ranging from 0 to 9 by a modification of a previous published protocol.[13] The grades assigned to each treatment group (mean ± SEM; $n = 4$/group) were compared for statistical significance using Mann-Whitney rank sum test.

Primary Rat RGCs Isolation

Primary cultures of rat RGCs were isolated according to the previously described two-step panning method.[14] Cells were cultured in a serum-free Dulbecco's modified Eagle's medium (DMEM; Invitrogen, Grand Island, NY, USA) containing brain-derived neurotrophic factor (BDNF, 50 ng/mL; Peprotech, Rocky Hill, NJ, USA), ciliary neurotrophic factor (CNTF, 10 ng/mL; Peprotech), and forskolin (5 ng/mL; Sigma-Aldrich Corp., St. Louis, MO, USA). Cells were incubated at 37°C in a humidified atmosphere of 10% CO_2 and 90% air. One week following culture, adherent RGCs with good neurite outgrowth were used for experiments.

In Vitro AAV Cell Transduction

Primary rat RGCs were infected with AAV encoding either GFP vector or Brn3b at 1×10^7 units per well. Cells were grown in complete serum-free DMEM containing BDNF (50 ng/mL), CNTF (10 ng/mL), and forskolin (5 ng/mL) in 5% CO_2 at 378°C. After 1 day, medium was replaced with fresh defined serum-free DMEM containing BDNF (50 ng/mL), CNTF (10 ng/mL), and forskolin (5 ng/mL). Medium was replaced every 2 days and cells were observed for hrGFP expression every other day. Maximum expression of hrGFP was detected by confocal imaging in primary ganglion cells and was observed 9 to 11 days following transduction.

Histology

Paraffin Sections. Saggital retinal sections through the optic nerve head (5-μm thick) were cut and deparaffinized in xylene (Fisher Scientific, NJ, USA), rehydrated using a

descending series of ethanol washes (100%, 95%, 90%, 80%, and 50% ethanol) and processed for immunohistochemical staining.

Cryosections. Animals were killed and eyes were enucleated and fixed in 4% paraformaldehyde for 3 hours. Fixed eyes and the eye-cups with optic nerve attached were embedded in optimal cutting temperature compound (OCT; Miles Diagnostics, Elkhart, IN, USA). Approximately 15-μm thick optic nerve and retinal sections were obtained. This technique was used specifically for CT-B tracing experiments. Optimal cutting temperature compound medium was removed by ethanol and water and slides were counterstained with DAPI before imaging. Sections were viewed with a Zeiss LSM 510 META confocal scanning microscope (Carl Zeiss Microscopy GmbH, Jena, Germany).

Immunocytochemistry and Immunohistochemistry Analysis

Immunohistochemistry. The deparaffinized and rehydrated retinal and optic nerve head sections were blocked with 5% normal donkey serum and 5% BSA in PBS and treated with primary antibodies: custom-made rabbit anti-Brn3b (1.5 μg/mL; Antibody Research Corporation, St. Charles, MO, USA), rabbit anti-GAP-43 (diluted 1:250; Sigma-Aldrich Corp.) or mouse anti-GAP-43 (diluted 1:500; Sigma-Aldrich Corp.), mouse anti-acetylated α-tubulin (ac-Tuba, diluted 1:3000; Sigma-Aldrich Corp.), rabbit anti–actin-binding LIM protein (abLIM, diluted 1:50; Sigma-Aldrich Corp.), and incubated for 1 hour at room temperature. Secondary incubation for 1 hour was carried out with a 1:1000 dilution of the appropriate secondary antibody conjugated with Alexa (546 or 647; Molecular Probes, Eugene, OR, USA). Sections in which the primary antibody incubation was excluded served as blanks and were used to assess nonspecific staining by the secondary antibody. All sections were stained with DAPI to visualize nuclei. Fluorescence images were taken in a Zeiss LSM 510 META confocal microscope.

Immunocytochemical Analysis of Primary RGCs. Primary retinal ganglion cells were grown on coverslips and fixed with 100% methanol/acetone at −20°C. Nonspecific binding was blocked with solution of 5% normal donkey serum in PBS at room temperature and treated with primary antibodies: custom made rabbit anti-Brn3b (1.5 μg/mL; Antibody Research Corporation, St. Charles, MO, USA) and mouse anti-GAP-43 (diluted 1:500; Sigma-Aldrich Corp.) for 1 hour at room temperature. Secondary antibodies (Alexa Fluor 547, Alexa Fluor 647, 1:1000 dilution; Invitrogen) were added and incubated for 1 hour at room temperature. Cells were imaged in a Zeiss confocal laser scanning microscope LSM 510.

Immunoblot Analysis of Optic Nerve Extracts. Total whole rat optic nerve homogenate were prepared in ice-cold TM buffer (10 mM HEPES buffer, pH 7.9, 1.5 mM $MgCl_2$, 10 mM KCl, 200 mM sucrose, 10% glycerol, 1 mM EDTA, 1% NP-40, 0.5% sodium deoxycholate, and 1.5 mM sodium orthovanadate, and Complete Protease Inhibitor Cocktail; Roche, San Francisco, CA, USA). The extracts were separated by SDS-PAGE and immunoblot analysis was carried out using specific antibodies including rabbit anti-GAP-43 (diluted 1:500; Sigma-Aldrich Corp.), rabbit anti-abLIM (diluted 1:500; Sigma-Aldrich Corp.), rabbit anti-NF-M (diluted 1:1000; Sigma-Aldrich Corp.), and rabbit anti-calnexin (diluted 1:5,000; Stressgen, Ann Arbor MI, USA). Donkey anti-rabbit IgG horseradish peroxidase (HRP) conjugate (GE Healthcare Bio-Sciences, Piscataway, NJ, USA) were used as the secondary antibody (1:10,000 dilution). The blots were developed with the enhanced chemiluminescence (ECL) reagents as per the manufacturer's instructions (GE Healthcare Bio-Sciences). The chemiluminescent bands from the blots were analyzed using the Molecular Imager Chemi Doc XRS+ Imaging system (Bio-Rad, Hercules, CA, USA). The band intensities of individual proteins were normalized to the corresponding calnexin band intensity in each blot. Calnexin was chosen as a loading control in immunoblotting as previously published.[15–22] Mean values ± SEM were obtained from ratios of normalized band intensities between treated IOP-elevated left (L) eye and untreated (contralateral) right (R) eye.

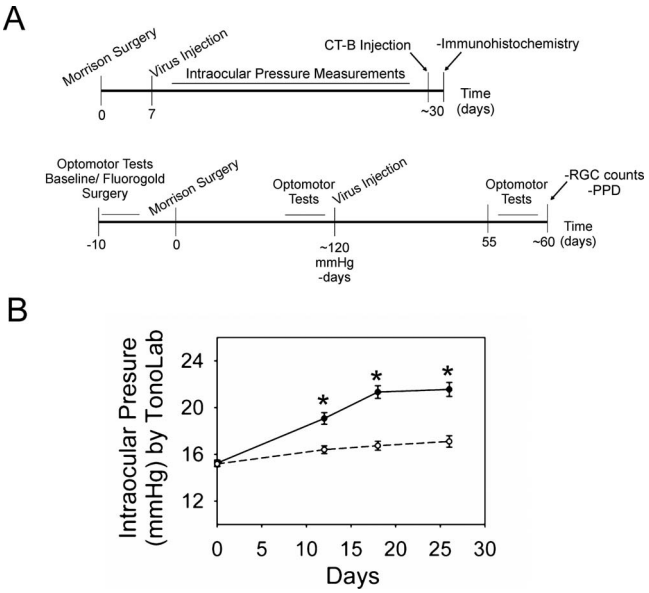

Figure 2. Administration of viral vectors following IOP elevation by the Morrison's method in Brown Norway rats. (**A**) Experimental scheme: IOP was elevated in one eye of Brown Norway rats using the Morrison's method followed by intravitreal injection of either rAAV-CMV-GFP or rAAV-CMV-Brn3b (1×10^9 particles per eye). Intraocular pressure measurements were carried for 3 weeks following the virus injection after which, the Brown Norway rats were killed. Some experimental groups of rats were additionally injected with Alexa-fluor 555 conjugated Cholera Toxin subunit B (CT-B; 48 hours prior to euthanization) to assess axonal transport changes. In a separate set of experiments, following baseline measurements of optomotor tests, RGCs were retrogradely labeled with Fluorogold in Brown Norway rats. Intraocular pressure elevation was carried out in one eye of the rats by the Morrison's method and rats were maintained for 4 to 6 weeks (until an IOP exposure of 120 mm Hg-days was obtained). Optomotor testing was carried out to determine changes in visual acuity after IOP elevation. rAAV-hsyn-GFP or rAAV-hsyn-Brn3b viruses (1×10^9 particles per eye) were injected in the IOP-elevated eye and maintained for an additional 4 weeks. Optomotor tests were continued to assess the effect of Brn3b overexpression on visual acuity in IOP-elevated rat eyes. Rats were killed and retinal flat mounts were prepared and RGC counts were obtained. Optic nerve sections obtained from the rats were stained with PPD to assess integrity of the optic nerve. Total number of rats tested was $n = 14$ for Brn3b protein overexpression and $n = 15$ for control vector. (**B**) Intraocular pressure elevation profile in Brown Norway rats. Intraocular pressure was elevated in one eye of adult male Brown Norway rats using the Morrison's method following which AAV-2 viruses were administered. Intraocular pressure values were obtained and plotted as mean ± SEM (*solid line*, IOP-elevated and virus-injected eye; *dashed line*, untreated contralateral eye). *Asterisk* indicates $P < 0.001$ statistical significance of the IOP-elevated IOP eye compared with contralateral eye using a *t*-test.

Immunoblot Analysis of Primary RGCs. The cells were lysed using RIPA buffer with proteinase inhibitors cocktail (Roche), sonicated and spun down at 4°C at 16,000*g* for 3 minutes. Immunoblot analyses to detect specific proteins of interest were carried out using the following antibodies: rabbit anti-GAP-43 (diluted 1:500; Sigma-Aldrich Corp.), rabbit Anti-

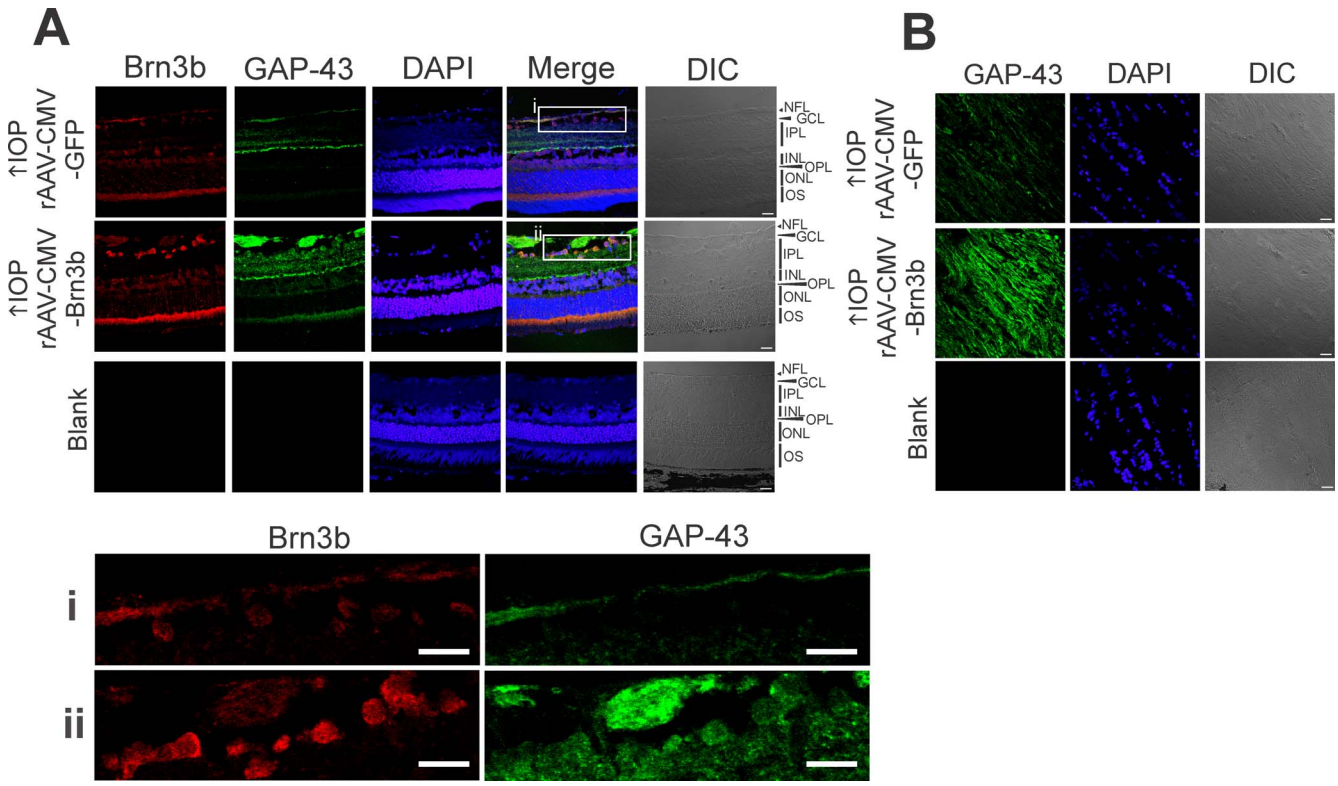

Figure 3. Transcription factor Brn3b-mediated increase in growth cone marker, GAP-43, in the retina and optic nerve head of IOP-elevated Brown Norway rats. (**A**) Brn3b (*pseudo-red*) and GAP-43 (*pseudo-green*) expression in retinal sections from IOP-elevated Brown Norway rat eyes injected with either rAAV-CMV-GFP (vector control) or rAAV-CMV-Brn3b virus, detected with secondary antibodies conjugated with Alexa 555 or 647 dye. Insets ([**i**] rAAV-CMV-GFP, [**ii**] rAAV-CMV-Brn3b) show higher magnification of RGC and NFLs of transduced retinas. (**B**) Immunohistochemical analysis of GAP-43 protein expression (*pseudo-green*) posterior to the optic nerve head of IOP-elevated rats following administration of the rAAV-CMV-GFP or rAAV-CMV-Brn3b. Retinal sections incubated with the secondary antibody alone (after excluding the primary antibody) showed minimal staining (Blank). *Scale bars*: 20 μm.

POU4F2 (diluted 1:1000; GenWay Biotech, Inc., San Diego, CA, USA), rabbit anti-Flag (diluted 1:1000; Sigma-Aldrich Corp.), and normalization was done using rabbit anti-calnexin (diluted 1:5000; Cell Signaling Technology, Danvers, MA, USA). Anti-rabbit or anti-mouse IgG HRP conjugate (GE Healthcare Bio-Sciences) were used as the secondary antibody (1:10,000 dilution) for detection of binding of the primary antibody. The blots were developed with the ECL reagents as per manufacturer's instructions (GE Healthcare Bio-Sciences). The bands observed in the images were analyzed by Molecular Imager Chemi Doc XRS+ Imaging system (Bio-Rad).

Adult Rat Retinal Explants

Adult female Sprague-Dawley rat retinal explants were prepared by making 2-mm punches in retinas isolated from each eye and placed on coverslips coated with poly D-lysine/mouse-laminin (Trevigen, Inc., Gaithersburg, MD, USA) with the outer retinal surface facing up. The explants were maintained at 5% CO_2 at 37°C in a culture medium comprising of Neurobasal-A medium supplemented with B27, N2, penicillin/streptomycin, and L-glutamine (Life Technologies, Grand Island, NY, USA). For transduction of rat retinal explants AAV serotype 2 viruses (manufactured by Penn Vector Core, Philadelphia, PA, USA) rAAV-hsyn-GFP and rAAV-hsyn-Brn3b were used. Explants were transduced with AAV viruses (1×10^8 GC units per well/explant). The protein expression from viral constructs started at day 3 of ex vivo culture. One-half the retinal explant culture medium was changed every second day and live imaging of neurite outgrowth was carried out in a EVOS-FL Digital Fluorescence Microscope under 20× magnification with transmitted light, at room temperature, following 5 and 7 days of ex vivo culture ($n = 7$ for each treatment group). The average length of neurites was calculated using ImageJ software (http://imagej.nih.gov/ij/; provided in the public domain by the National Institutes of Health, Bethesda, MD, USA) with NeuronJ plugin and statistically significant differences were assessed using Mann-Whitney rank sum test using SigmaPlot software (Systat Software, Inc., San Jose, CA, USA).

In another set of experiments retinal explants were transduced with rAAV-hsyn-GFP or rAAV-hsyn-Brn3b viruses (1×10^8 GC units per well\explant). After 6 days of ex vivo culture, retinal explants were fixed with 4% phosphate-buffered paraformaldehyde for 1 hour, rinsed three times in PBS, pH 7.5 and blocked for 1 hour with blocking buffer (5% normal donkey serum and 5% BSA in 1× PBS). The explants were tested for expression of a RGC-specific marker, β-III tubulin[23] using a mouse anti β-III tubulin antibody (Sigma-Aldrich Corp.) for 3 hours. After washing three times with PBS, incubation with a fluorescently-labeled secondary antibody (donkey anti-mouse Alexa 647; Invitrogen; and donkey anti-rabbit Alexa 546; Invitrogen) was carried out for 2 hours and mounted with ProlongGold with DAPI (Invitrogen). The retinal explants from three experiments ($n = 6$ explants/treatment group) were visualized using Zeiss LSM 510 Meta scanning confocal microscope. Brightness and contrast levels were maintained at the same setting for all the fluorescent images. The number of β-III tubulin–positive cells in each immunostained explants was counted using ImageJ software, cell counter plugin and statistical differences were

Investigative Ophthalmology & Visual Science

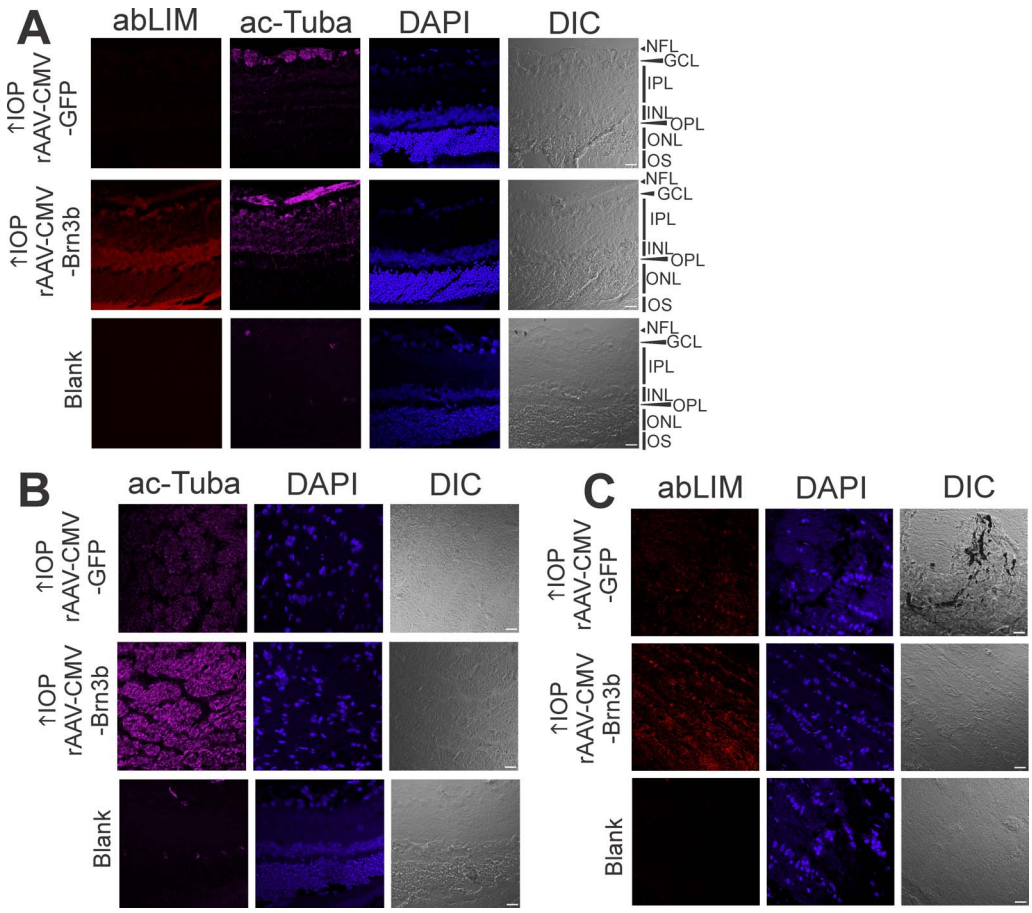

Figure 4. Transcription factor Brn3b promotes an increase in markers of axonal integrity including actin-binding LIM protein (abLIM) and acetylated α tubulin (ac-Tuba). (**A**) Immunostaining for abLIM and ac-Tuba in retinas of Brown Norway rats intravitreally injected with either rAAV-CMV-GFP or rAAV-CMV-Brn3b following IOP elevation. (**B**) Increased immunostaining for ac-Tuba, was observed in the posterior region of the optic nerve head in IOP-elevated– and rAAV-CMV-Brn3b–injected rats compared with that seen in IOP-elevated–and rAAV-CMV-GFP–injected rats. (**C**) AbLIM immunostaining in the retrolaminar region of the optic nerve head was modestly increased following AAV mediated Brn3b protein overexpression in ocular hypertensive rats. Binding of primary antibodies was detected with appropriate secondary antibodies conjugated with Alexa 555 (*pseudo-colored magenta*) or 647 (*pseudo-colored red*) dye. A negative control immunostaining (Blank), in which the primary antibody was excluded, showed minimal staining. Cells were counterstained with DAPI (*blue*) to detect cell nuclei. *Scale bars*: 20 μm.

calculated using Mann-Whitney rank sum test using SigmaPlot software (Systat Software, Inc.).

Results

Increased Levels of Brn3b and GAP-43 in Primary RGCs Transduced With the rAAV-CMV-Brn3b Virus

Primary RGCs were obtained from postnatal day 5 rat pup eyes and used to test the ability of AAV to transduce the RGCs. As shown in Figure 1A, RGCs transduced with either with rAAV-CMV-GFP (control vector) or rAAV-CMV-Brn3b (encoding transcription factor Brn3b) viral constructs showed expression of *Renilla reniformis* hrGFP from the bicistronic viral construct, 11 days post transduction. rAAV-CMV-Brn3b virus was also found to be capable of overexpressing the Brn3b protein in RGCs, as seen by increased immunostaining for Brn3b (Fig. 1B, pseudo-red), compared with those infected with rAAV-CMV-GFP virus. Brn3b protein overexpression in primary RGCs also produced increased labelling for the growth cone-enriched protein, growth associated protein-43 (GAP-43; Fig. 1B, pseudo-green). Transgene expression of Brn3b was detected by immunoblotting using a Flag-tag antibody (Fig. 1C). In addition, immunoblot analysis of primary RGCs also showed a significant increase in Brn3b protein level in the rAAV-CMV-Brn3b transduced group in comparison with the rAAV-CMV-GFP transduced RGCs (Fig. 1C). Normalized densitometric analysis of the Brn3b bands showed a 3-fold increase in rAAV-CMV-Brn3b transfected RGCs, compared with those of rAAV-CMV-GFP transfected RGCs. Similar to the immunocytochemistry data, upregulation of Brn3b protein promoted a 2-fold increase in GAP-43 levels as determined by immunoblotting (Fig. 1C). Calnexin, an endoplasmic reticulum integral membrane protein, was used as a loading control was not appreciably different between the various experimental groups.

Experimental Scheme and IOP Elevation Profile in an Ocular Hypertension Glaucoma Model in Brown Norway Rats

A brief outline of the experimental scheme for this study is provided in Figure 2A. Studies were carried out using a total of 29 male retired breeder Brown Norway rats (*R. norvegicus*) according to the scheme depicted in Figure 2A. Intraocular pressure was elevated using the Morrison's surgical method in one eye of Brown Norway rats, while the corresponding contralateral eye was left untreated.[10,24] After surgery to

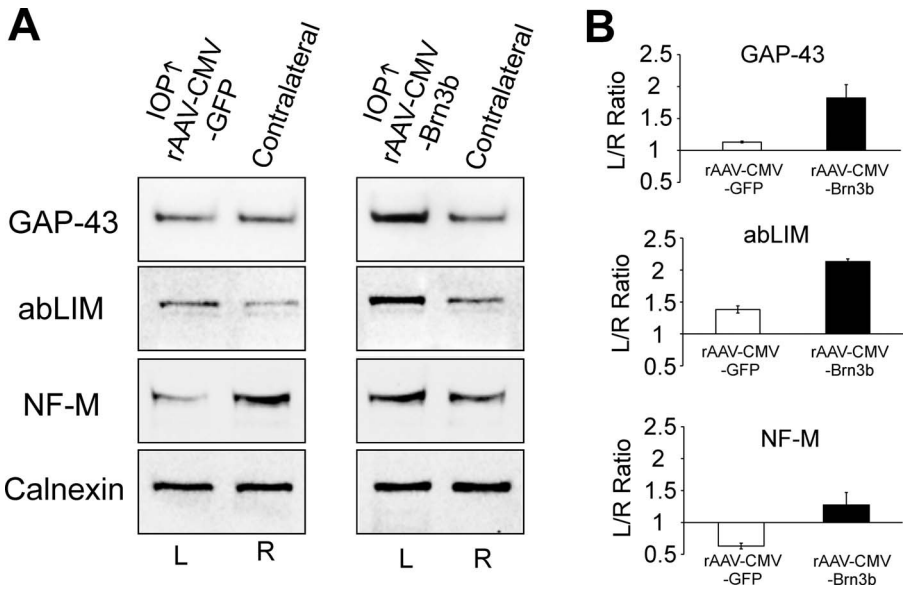

Figure 5. rAAV-CMV-Brn3b administration increased expression of GAP-43, abLIM, and neurofilament-M proteins following IOP elevation in Brown Norway rats. (**A**) Intraocular pressure was elevated in the left eye of Brown Norway rats while the contralateral right eye served as the corresponding control. Immunoblots of whole optic nerves extracts, obtained 3 weeks following rAAV-CMV-GFP or rAAV-CMV-Brn3b virus injection into IOP-elevated left eye (IOP↑) of Brown Norway rats. Blots were probed with specific antibodies against GAP-43, abLIM, and neurofilament-M (NF-M). Calnexin served as a loading control. (**B**) Intraocular pressure–elevated Left(L)/Contralateral Right (R) ratio of densitometry readings (normalized to corresponding calnexin levels) representing ratio between IOP-elevated and contralateral eye are presented as mean ± SD.

elevate IOP, the Brown Norway rats were maintained for 7 to 10 days and injected intravitreally in the IOP-elevated eye with 1×10^9 AAV particles encoding either the control vector (rAAV-CMV-GFP) or the transcription factor Brn3b (rAAV-CMV-Brn3b) and maintained for an additional period of 3 weeks. Intraocular pressure was measured using the Tonolab tonometer and plotted as a function of time. The extent of IOP exposure was computed in millimeter per mercury per days. In separate experiments, some rats were injected 48 hours prior to euthanasia with the anterograde axonal transport tracer, Alexa-fluor 555–conjugated cholera toxin subunit B (CT-B).

In a different group of rats, RGCs were retrogradely labeled with fluorogold, following which IOP was elevated in one eye, while the other eye served as the contralateral control. After maintaining rats to an IOP exposure of approximately 120 mm Hg-days, the rats were injected in the IOP-elevated eye with either rAAV-hsyn-GFP or rAAV-hsyn-Brn3b virus. Following an additional 4 weeks, rats were killed, optic nerve sections, and retinal flat mounts were obtained and imaged. In this group of rats, optomotor tests were carried out to determine visual acuity of rats following various treatments.

As seen in Figure 2B, IOP was elevated after 7 to 10 days following surgery and remained elevated for the entire duration of the experiment. Intraocular pressure values (n = 29 rats) were plotted as mean ± SEM (Fig. 2B). Intraocular pressure elevation for 3 weeks typically generated 74 to 104 mm Hg-days of IOP exposure (the difference of the area under the curve between IOP-elevated eye and contralateral eye).

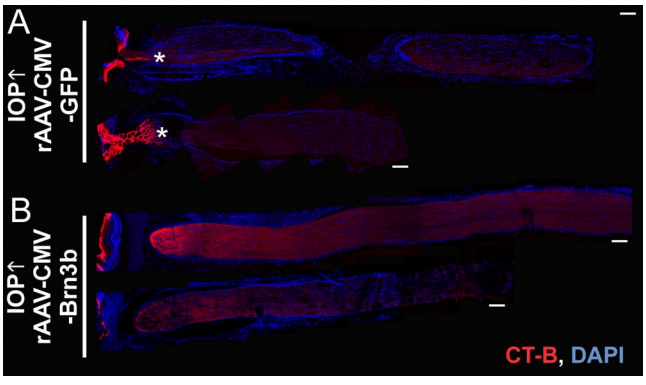

Figure 6. Overexpression of transcription factor Brn3b caused amelioration of axonal transport indicative of recovery from axonal injury in an elevated-IOP rat model of glaucoma. Assessment of axonal transport in Brown Norway rats in which either the control viral vector (rAAV-CMV-GFP) or the rAAV-CMV-Brn3b vector was administered following IOP elevation. Anterograde axon transport was detected using the anterograde axonal tracer Alexa555-conjugated cholera toxin subunit B (CT-B). All the rats were injected with CT-B (*pseudo-red*), 48 hours prior to euthanization. DAPI staining (*blue*) indicates nuclei of cells. *Scale bars*: 250 μm. (**A**) A block of axonal transport of CT-B was observed close to the site of optic nerve injury (indicated by *) in rAAV-CMV-GFP vector injected rats (n = 5). (**B**) Enhanced staining for the anterograde tracer along the optic nerve, past the transition zone in Brown Norway rats (n = 5) injected with rAAV CMV Brn3b vector. A robust staining for CT-B was seen past the transition zone into the myelinated portion of the optic nerve.

Increased Level of the GAP-43 Protein in the Retina and Optic Nerve Head Following IOP Elevation and Administration of rAAV-CMV-Brn3b in Brown Norway Rats

Injection of hypertonic saline through episcleral veins by the Morrison's method was used to elevate IOP in one eye of Brown Norway rats. One week following surgery, viral vectors (rAAV-CMV-GFP or rAAV-CMV-Brn3b) were injected intravitreally into the IOP-elevated eye. The rats were maintained for 3 weeks following virus injection and killed. Rat retina sections through the optic nerve heads were obtained and subjected to immunohistochemistry to detect Brn3b and GAP-43 protein levels. As seen in Figure 3A, increased Brn3b immunostaining (pseudo-red) was detected in rAAV-CMV-Brn3b administered rat retinas mainly in GCL and nerve fiber layer (NFL), with lower levels also detected in the inner nuclear layer (INL) and

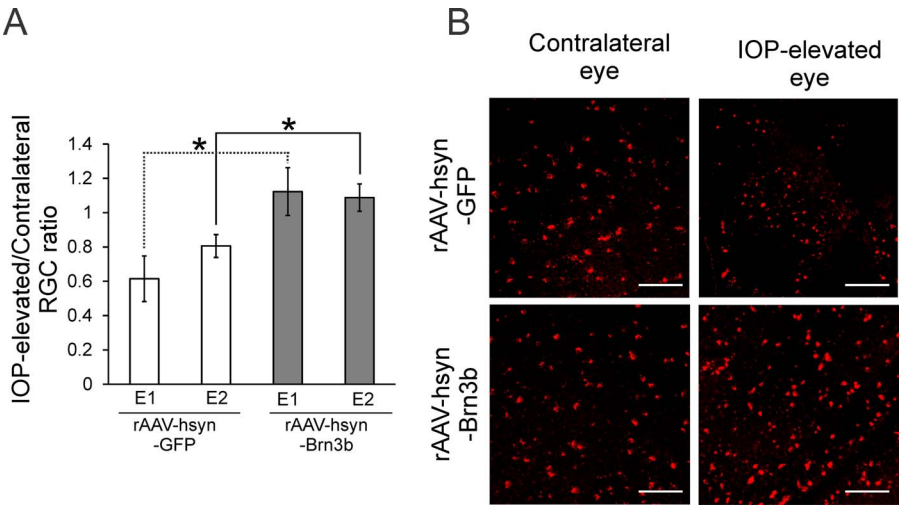

Figure 7. Neuroprotection of RGCs in rAAV-hsyn-Brn3b–treated rat eyes, compared with rAAV-hsyn-GFP–treated rat eyes following IOP elevation. (**A**) Male retired breeder Brown Norway rats were subjected to retrograde labeling of RGCs with fluorogold followed by elevation of IOP in one eye, while the other eye served as contralateral control. After IOP elevation, the operated eye was injected with either rAAV-hsyn-GFP or rAAV-hsyn-Brn3b and maintained for 1 month and killed. Retinal ganglion cells were counted at two eccentricities located 2/sixth (E1) and 4/sixth (E2) from the optic nerve head. A significant ($^*P < 0.05$, $n = 4$ per group, *t*-test) neuroprotection of RGCs was observed in both eccentricities (E1 and E2) in retinas from rat eyes administered with the rAAV-hsyn-Brn3b virus, compared with the corresponding eccentricities from rAAVhsyn-GFP–injected rat eyes. (**B**) Representative fluorescent images of retrograde labeled RGCs in contralateral and IOP-elevated rat retinas transduced either with rAAV-hsyn-GFP or rAAV-hsyn-Brn3b. *Scale bars*: 250 μm.

the outer segment (OS). Ectopic Brn3b localization in the outer retina has also been observed in an earlier studies.[25–28] Interestingly, GAP-43 protein (pseudo-green) was upregulated most prominently in the NFL, and enhanced staining was also observed in GCL and inner plexiform layer (IPL) of the retina in rAAV-CMV-Brn3b injected rat eyes. Insets (Figs. 3Ai, 3Aii), showing higher magnification of ganglion cell and NFLs of retinas indicate increased staining of Brn3b and GAP-43 in retinal ganglion cells in rAAV-CMV-Brn3b–injected rat eyes compared with rAAV-CMV-GFP–injected rat eyes.

In the optic nerve head (Fig. 3B), a marked increase in GAP-43 immunostaining (pseudo-green) was detected posterior to the optic nerve head (in the retrolaminar region) in IOP-elevated rAAV-CMV-Brn3b–injected eyes in comparison with IOP-elevated rAAV-CMV-GFP–injected control eyes. Increased immunostaining for GAP-43 in IOP-elevated rAAV-CMV-Brn3b–injected rat eyes is an indicator of increased growth cone activity and synaptic plasticity at the site of injury. A negative control (Blank), in which the primary antibody was omitted, showed minimal staining, indicative of specificity of the immunostaining.

Markers of Axonal Integrity in the Retina and Optic Nerve Head of Rats Intravitreally Injected With the rAAV-CMV-Brn3b Following IOP Elevation in Brown Norway Rats

Since an increase in levels of GAP-43 was observed in Brown Norway rats injected intravitreally with the rAAV-CMV-Brn3b virus, additional studies were carried out to determine if markers of axonal integrity were upregulated in retinas and optic nerve heads of these rats. Briefly, IOP was elevated in one eye of Brown Norway rats, and 1 week following surgery, viral vectors encoding either GFP (rAAV-CMV-GFP) or Brn3b (rAAV-CMV-Brn3b) were administered to the IOP-elevated eyes. The animals were maintained for 3 weeks with IOP elevation and killed. Five-micron sagittal retina sections through the optic nerve head were obtained and analyzed by immunohistochemistry for the expression of markers of axonal stability/integrity, including acetylated α-tubulin (ac-Tuba) and actin-binding LIM protein (abLIM). An increase in abLIM was found in several retinal layers including GCL, INL, and OS compared with the control vector–injected rats eyes, where minimal staining for abLIM was found. One of the main regulators of axonal transport are posttranslational modifications of microtubules including acetylation of α-tubulin (ac-Tuba). Ac-Tuba has been extensively investigated in models of neurodegeneration. Acetylation of α-tubulin causes stabilization of the microtubule structure. Ac-Tuba promotes axonal transport by involving the motor proteins Kinesin-1 and cytoplasmic dynein to microtubules.[29,30] Inhibition of acetylation α-tubulin causes severe loss of kinesin heavy chain binding to the microtubules and significantly reduces speed of axonemes in neurons. An intense labeling for ac-Tuba was observed in NFL and GCL, and also in the inner plexiform layer (IPL) in IOP-elevated rats injected with rAAV-CMV-Brn3b, while a weaker staining was found in the NFL of IOP-elevated rats injected with rAAV-CMV-GFP virus (Fig. 4A).

An enhanced staining for ac-Tuba was observed posterior to the optic nerve head, in IOP-elevated rat eyes injected with rAAV-CMV-Brn3b virus, compared with those injected with control virus (Fig. 4B). A modest increase in immunostaining was also observed for abLIM posterior to the optic nerve heads of rAAV-CMV-Brn3b transduced rat eyes following IOP elevation, compared with those injected with rAAV-CMV-GFP (Fig. 4C). The data suggest that following IOP-mediated damage, overexpression of transcription factor Brn3b protein could upregulate markers of axonal integrity and possibly facilitate recovery from axonal injury, thereby promote neuroprotection.

Immunoblot Analysis of Markers of Axonal Integrity and Synaptic Plasticity in Optic Nerves Following IOP Elevation and Administration of rAAV-CMV-Brn3b in Brown Norway Rats

Since an enhanced immunostaining of GAP-43, abLIM, and ac-Tuba was observed in the retrolaminar region of the optic

nerve heads of IOP-elevated rAAV-CMV-Brn3b–injected rat eyes, compared with IOP-elevated control vector injected rat eyes (Figs. 3, 4), further analyses of these markers were carried out by immunoblotting of whole optic nerve extracts. The data obtained from immunoblots of optic nerve extracts from Brown Norway rats (Fig. 5A) confirmed the immunohistochemical analyses of GAP-43, and abLIM proteins. There was a modest 13% increase in GAP-43 in glaucomatous (IOP-elevated) optic nerves of rat eyes injected with rAAV-CMV-GFP virus compared with the level in contralateral control eyes. On the other hand, there was an 82% increase in GAP-43 levels in glaucomatous eyes injected with rAAV-CMV-Brn3b virus, compared with those of contralateral control eyes. Similar observations were made for abLIM in immunoblot analysis of optic nerve extracts. There was a minimal 6% increase in abLIM levels in rAAV-CMV-GFP virus injected, IOP-elevated eyes, compared with the corresponding contralateral eyes. In contrast, there was 217% increase in abLIM levels in IOP-elevated eyes injected with rAAV-CMV-Brn3b virus compared with the corresponding contralateral eyes.

Additionally, immunoblot analysis of neurofilament-M, one of the major intermediate filaments found in neurons, was carried out (Fig. 5A). Neurofilament M is the one of the components providing support for axonal radial growth and its expression increases in neuroregenerative responses.[31] Intraocular pressure elevation in conjunction with rAAV-CMV-GFP virus caused the major decrease in NF-M levels in rat optic nerves by approximately 40%, suggesting major axonal loss and degeneration. In rat eyes injected with rAAV-CMV-Brn3b following IOP elevation, NF-M levels showed a 27% increase in comparison to the values in the corresponding contralateral eyes. The ratios of band intensities (after normalizing with the corresponding loading control, calnexin) between IOP-elevated left (L) and contralateral control right (R) eyes in the two experimental groups (rAAV-CMV-GFP and rAAV-CMV-Brn3b injected) are presented as histograms in Figure 5B.

Axonal Transport in Optic Nerves of Rats Following IOP Elevation and Administration of rAAV-CMV-Brn3b

rAAV-CMV-Brn3b transduction produced increased levels of some synaptic plasticity and axonal integrity markers following IOP induced axonal damage in the optic nerve (Figs. 3–5). However, increase in synaptic plasticity markers is not indicative of functionality of the axons. To assess functional changes, axonal transport studies were carried out to determine if following IOP elevation, AAV-mediated Brn3b protein expression could ameliorate axonal transport that is disrupted due to injury to the optic nerve. Briefly, after IOP elevation and 3 weeks following administration of the viral vectors, rats were injected intravitreally with Cholera toxin B subunit (CT-B) Alexa Fluor 555 conjugate, which served as an anterograde transport tracer dye (scheme in Fig. 2A). The rats were killed 48 hours after administration of the anterograde tracer and 15-μm sagittal retina sections through the optic nerve head were obtained. The sections were imaged in a Zeiss confocal microscope to detect transport or accumulation of the CT-B along the axons of the optic nerve. It was found that IOP elevation produced an inhibition in axonal transport function, which was not affected by administration of the rAAV-CMV-GFP control virus, and most of the anterograde tracer CT-B was accumulated and retained in the anterior portion of the optic nerve head (anterior to the lamina-like region; Fig. 6A, indicated by [*] symbol). In some rAAV-CMV-GFP–injected rats, diffuse labeling for the CT-B was also observed along the superior and inferior poles of the optic nerve suggestive of a few intact axons active in axonal transport (Fig. 6A). This indicated that IOP elevation caused damage to the axons of optic nerve, thereby producing a decline in anterograde axonal transport.

On the other hand, optic nerve sections from IOP-elevated rAAV-CMV-Brn3b–injected rats revealed an appreciable increase in transport of CT-B tracer along the axonal tracts, which extended posteriorly beyond the site of axonal damage in the optic nerve head. The staining was traced up to the myelinated region of the optic nerve, indicative of a recovery from axonal injury and improvement of axonal transport, mediated by Brn3b overexpression (Fig. 6B).

Retinal Ganglion Cell Loss Was Attenuated in IOP-Elevated, rAAV-hsyn-Brn3b–Injected Rats

Intraocular pressure elevation in the Morrison rat model of ocular hypertension has been shown to produce significant RGC cell death and axonal loss.[32] To determine if transcription factor Brn3b has a neuroprotective role during ocular hypertension, Brown Norway rats were retrogradely labeled with Fluorogold, following which IOP elevation was carried out and maintained for approximately 120 mm Hg-days. The IOP-elevated eyes were injected with either rAAV-hsyn-GFP vector or rAAV-hsyn-Brn3b and maintained for an additional 4 weeks. After killing the animals, retinal flat mounts were isolated and RGC survival was assessed by counting fluorogold labelled, viable RGCs (Figs. 7A, 7B) in two eccentricities (E1 located 2/sixth and E2 located 4/sixth distance from the optic nerve head) within each retinal quadrant (superior, inferior, nasal, and temporal). The loss of RGCs was calculated as the ratio of RGC counts between IOP-elevated and contralateral eye for each eccentricity. The obtained ratios were then compared between rAAV-hsyn-GFP and rAAV-hsyn-Brn3b–treated animals and plotted as a mean ± SEM (Fig. 7A). The ratios of RGC counts were significantly higher in rAAV-hsyn-Brn3b–injected rats in both eccentricities, compared with those of the rAAV-hsyn-GFP–injected rats. This suggests that following IOP elevation AAV-mediated expression of the transcription factor Brn3b plays a neuroprotective role, helping to sustain the viability of RGCs.

Axonal Integrity in IOP-Elevated, rAAV-hsyn-Brn3b–Injected Rat Eyes

Since a significant protection of RGCs somas was observed in rAAV-hsyn-Brn3b administered rats following IOP elevation, compared with rAAV-hsyn-GFP–treated IOP-elevated rats, optic nerve axonal integrity was assessed in these groups of animals. Intraocular pressure was elevated in one eye of Brown Norway rats, while the corresponding contralateral eye served as control. After IOP elevation, rats were maintained till an IOP exposure of approximately 120 mm Hg-days was obtained, following which the animals were intravitreally injected either with rAAV-hsyn-GFP or rAAV-hsyn-Brn3b vectors into the IOP-elevated eyes. After maintaining for 4 weeks, Brown Norway rats were killed, optic nerve sections were obtained and stained with PPD. As shown in Figure 8A, a compromise of axonal integrity and a loss of axonal bundles was observed in optic nerve sections from IOP-elevated rAAV-hsyn-GFP–injected rats. In contrast, optic nerve sections from IOP-elevated rAAV-hsyn-Brn3b–injected rats showed an enhanced preservation of axon morphology (Fig. 8A). Optic nerve grading was done by masked observers according to the method described by Chauhan et al.[13] Grade 0 was assigned to optic nerves without any damage with all the nerve bundles intact, while grades 3 and 6 correspond to 30% and 60% of mean axonal damage. There was statistical difference between the integrity

Investigative Ophthalmology & Visual Science

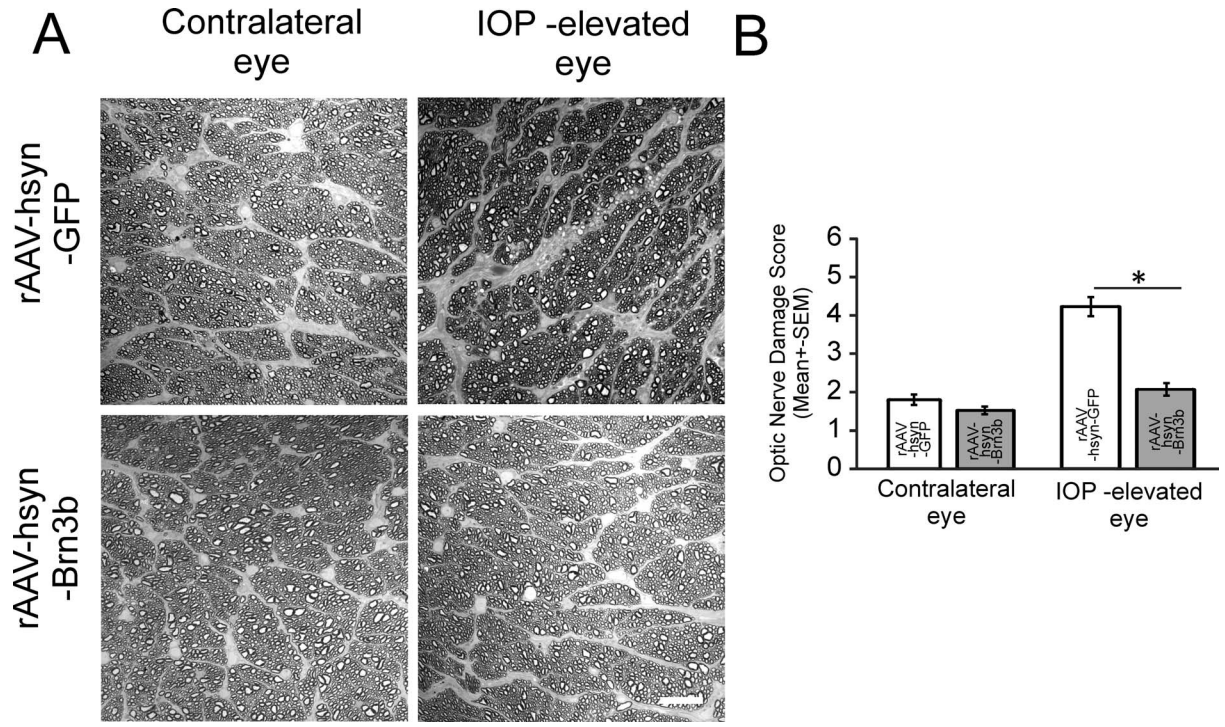

Figure 8. Survival of optic nerve axons in rAAV-hsyn-Brn3b transduced rat eyes, compared with rAAV-hsyn-GFP transduced rat eyes following IOP elevation. Intraocular pressure was elevated in one eye of rats, while the other eye served as corresponding contralateral control. The rats were maintained for 120 mm Hg-days of IOP elevation and injected either with rAAV-hsyn-GFP or rAAV-hsyn-Brn3b viruses. Rats were killed following another 4 weeks and optic nerve sections were stained with PPD. (**A**) Representative bright field images of PPD-stained optic nerves. An appreciable loss of axon bundles was observed in IOP-elevated, rAAV-hsyn-GFP–injected rat eyes, which was attenuated in the IOP-elevated, rAAV-hsyn-Brn3b administered rat eyes. *Dark spots* indicate dying/degenerating axons. *Scale bar*: 20 μm. (**B**) Plot of the optic nerve damage scores following optic nerve grading by masked observers ($n = 7$/group). $^{*}P < 0.005$ by Kruskal-Wallis one way analysis of variance on ranks test.

scores of optic nerves between contralateral, noninjected as well IOP-elevated eyes of the rAAV-hsyn-GFP– and rAAV-hsyn-Brn3b–injected rats (Fig. 8B). These results suggest that AAV-mediated expression of the Brn3b transcription factor following the initial IOP damage have neuroprotective effects on the axons of the optic nerve in addition to protecting RGCs from cell death.

Visual Acuity in IOP-Elevated Rat Eyes Following Administration of rAAV-hsyn-Brn3b

To determine if there is an improvement of visual function in rats administered with the rAAV-hsyn-Brn3b viral vector following IOP elevation, a behavioral test was performed using the visual optomotor response (mediated by a subcortical reflex) in which an animal reflexively follows a moving visual stimulus with its eyes, thereby compensating for rotation of the visual field.

The baseline acuity in both eyes of Brown Norway rats was characterized before evaluating the effects of IOP elevation and AAV treatments. Baseline values of visual acuity of adult Brown Norway rats obtained (Fig. 9) were comparable with those of normal Long-Evans pigmented rats previously published by Douglas and colleagues[33] using the same OptoMotry testing apparatus and ranged between 0.619 (c/d) ± 0.0134 and 0.648 (c/d) ± 0.0213.

Rats were again administered optomotor testing following approximately 120 mm Hg-days of IOP elevation, following which the rAAV-hsyn-GFP ($n = 7$ rats) or rAAV-hsyn-Brn3b viruses ($n = 7$ rats) were intravitreally injected. Each rat was tested between three and four times in separate sessions in a

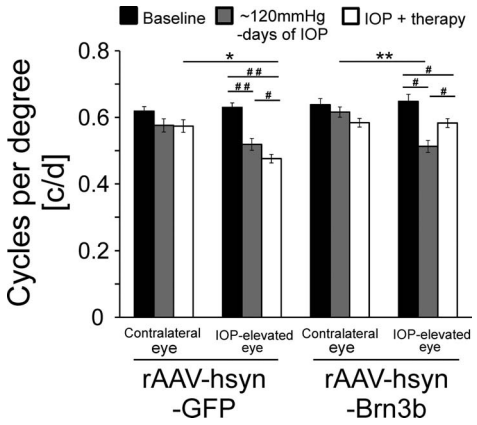

Figure 9. Recovery of visual acuity in IOP-elevated eyes treated with rAAV-hsyn-Brn3b. Following IOP elevation and rAAV-hyn-GFP virus injection, acuity of the IOP-elevated eye (operated eye, *gray bars*) was reduced in comparison with the contralateral eye. There was a progressive decline in visual acuity after rAAV-hsyn-GFP vector treatment (*white bar*) due to persistent IOP elevation. Visual acuity of the IOP-elevated and rAAV-hsyn-Brn3b–treated eyes was partially restored after treatment (*white bar*). The baseline measurements of visual acuity from the left and right eyes for both groups were not statistically different prior to the experiment. Comparison between contralateral and operated eyes was done using *t*-test: $^{**}P < 0.001$, $^{*}P < 0.002$. To assess the differences before and after IOP elevation and following AAV treatment, the paired *t*-test was used: $\#\#P < 0.001$, $\#P < 0.05$ ($n = 7$/experimental group).

masked manner, and the average acuity measured as cycles per degree from these sessions was used in the analyses. Rats were killed following 4 weeks after AAV administration. Compared with baseline values, visual acuity (cycles/degree) was significantly decreased in all rats that were subjected to 120 mm Hg-days of IOP elevation (Fig. 9, gray bars, IOP-elevated eyes). Visual acuity of rats receiving rAAV-hsyn-GFP virus treatment for 4 weeks following IOP elevation was further reduced in comparison to just IOP elevation ($P < 0.05$) and to baseline ($P < 0.001$; Fig. 9, white bars, IOP-elevated eyes). Thus, the IOP elevation produced the expected deficit in visual function. However, rAAV-hsyn-Brn3b delivery to IOP-elevated rat eyes (Fig. 9, white bar) resulted in some recovery of visual acuity in comparison to IOP elevation ($P < 0.05$), although not to the level of baseline values ($P < 0.05$). Based upon these observations it appears that the rAAV-hsyn-Brn3b treatment was successful in partially restoring visual function following IOP-mediated damage to the optic nerve.

rAAV-hsyn-Brn3b Mediated Neurite Outgrowth and Neuroprotective Effects in Adult Rat Retinal Explants

We determined the neuroprotective effects of rAAV-hsyn-Brn3b overexpression on RGCs in adult retinal explants. After 6 days of ex vivo culture of retinal explants followed by fixation and immunostaining, visualization of RGCs was performed, using antibody to the RGC-specific marker β-III tubulin (Fig. 10A). Increase in β-III tubulin levels was observed in retinal explants transduced with rAAV-hsyn-Brn3b compared with rAAV-hsyn-GFP. The insets (Figs. 10Ai, 10Aii) show magnification of β-III tubulin–labeled RGCs. The number of β-III tubulin–positive cells in rAAV-hsyn-Brn3b transduced explants ($n = 6$ from three experiments) was 1812.73 ± 119.11 per mm^2 (mean ± SEM) in comparison to 990.30 ± 66.04 per mm^2 (mean ± SEM) that was observed in rAAV-hsyn-GFP explants ($n = 6$; Fig. 10B). The cell counts in the Brn3b transduced explants were significantly higher than those of rAAV-hsyn-GFP explants (*$P \leq 0.001$) by Mann-Whitney rank sum test.

Further experiments were carried out to determine if AAV-mediated expression of Brn3b protein was sufficient for promoting neurite outgrowth in retinal explants from adult rats (Fig. 10C). To test this hypothesis, rat retinal explants, maintained without trophic factors were transduced either with rAAV-hsyn-GFP or rAAV-hsyn-Brn3b viruses and evaluated 5- and 7- days ex vivo. Cultured retinal explants transduced with rAAV-hsyn-GFP virus at day 5 did not extend more than average 2.8 processes per field of view (magnification ×20). On the other hand, rAAV-hsyn-Brn3b transduced explants grew an average of five processes per field of view at the same magnification. After maintaining for 7 days ex vivo, and rAAV-hsyn-Brn3b continued to have higher number of neurites (average of 4.5 neurites), compared with those of rAAV-hsyn-GFP (average of 1.5 neurites per field of view). As seen in Figure 10D, the length of processes originating from each cultured retinal rAAV-hsyn-Brn3b transduced explants ($n = 7$) was 3.0 ± 0.35 (mean ± SEM) times longer than in explants ($n = 7$) transduced with rAAV-hsyn-GFP virus. Statistical differences were significant in three independent experiments for rAAV-hsyn-GFP explants compared with rAAV-hsyn-Brn3b explants (*$P \leq 0.001$; Mann-Whitney rank sum test).

Discussion

Glaucoma treatment comprises mainly of approaches to lower IOP either surgically or through IOP lowering drugs that act by reducing aqueous humor formation or increasing its outflow. However, neurodegeneration continues to occur slowly despite these treatments, hence, there is a need for developing neuroprotective strategies in addition to lowering IOP. Neuroprotection is an important area of glaucoma research, which has made appreciable progress in the light of key findings that demonstrate neuroprotective effects in the retina and optic nerve in animal models of optic neuropathy.[34] In the current study, we employed a rat model of optic neuropathy in which elevation of IOP was carried out followed by administration of an AAV vector encoding Brn3b to test its efficacy to promote neuroprotection. Adeno-associated virus vectors have been shown to be safe and efficacious for use in humans and hold promise for future therapies.[35–38] Transcription factor Brn3b plays a crucial role during development and differentiation of RGCs, as evidenced by loss of nearly 70% of RGCs in Brn3b-deficient mice. Deletion of either Brn3a or Brn3c does not greatly affect retinal neurons and appears to cause loss of dorsal root ganglion neurons and vestibular hair cells, respectively.[4,8] The status of Brn3b in neurodegeneration as well as its potential role in promoting neuroprotection is largely unclear. Intraocular pressure elevation in rats using the Morrison's method has been shown to produce damage to optic nerve axons and progressive death of RGCs, with nearly 30% loss after 4 weeks of IOP elevation.[39]

Use of Brn3b as a therapeutic agent could have minimal undesirable effects, since Brn3b is endogenously expressed in adult retinas and different parts of the brain, including superior colliculus, interpeduncular nucleus, or trigeminal ganglion.[40] Brn3b is also constitutively expressed in mature RGCs suggestive of its putative role in normal RGC physiology, which is not completely understood. A decrease in Brn3b expression has been demonstrated in different animal models of glaucoma, suggesting that downregulation of Brn3b precedes neurodegeneration. For instance, several investigators reported that a decrease in Brn3b protein occurs prior to apoptosis of RGCs in an optic nerve injury model in rats.[41–43]

One of the important axon outgrowth regulators is GAP-43, which is known to be enriched in growth cones and in the presynaptic terminals in areas of high plasticity.[44] GAP-43 has been shown to be expressed by RGCs during cell development and axonal outgrowth[45,46] and is known to be significantly downregulated after the development of the eye.[47] Mu et al.[48] showed that expression of GAP-43 is attenuated in Brn3b knockout mice compared with wild type suggesting a regulatory linkage between the transcription factor Brn3b and expression of GAP-43. In the present study, we demonstrate that AAV-derived Brn3b is able to increase levels of GAP-43, which could indicate new growth cone formation posterior to the optic nerve head. We also investigated the status of other synaptic plasticity markers after IOP elevation and AAV-directed expression of Brn3b.

Growth cone formation and synaptic plasticity depend largely on cytoskeletal dynamics. Microtubules, comprised of polymers of alpha and beta tubulin dimers, are the essential components of the cytoskeleton required for axonal growth and transport. In particular, acetylation of α-tubulin has been shown to be associated with stable microtubule structures, which are essential for axon elongation. In previous studies, an analysis of brain-derived neurotrophic factor (BDNF) vesicles in primary cortical neurons from P0 rats demonstrated that acetylation of the α-tubulin stimulates anterograde as well as retrograde axonal transport.[30,49] Total tubulin mRNA levels were low after injury in the optic nerve but increased in those RGCs that regenerated their axons.[50] Low concentrations of the chemotherapeutic agent Taxol have been shown to promote acetylation of α-tubulin and neurite elongation of RGCs in culture.[51] Moreover, inhibition of tubulin deacetylase has been demonstrated to have a proregenerative response in CNS.[52] These data indicate that acetylation of tubulin helps to

Investigative Ophthalmology & Visual Science

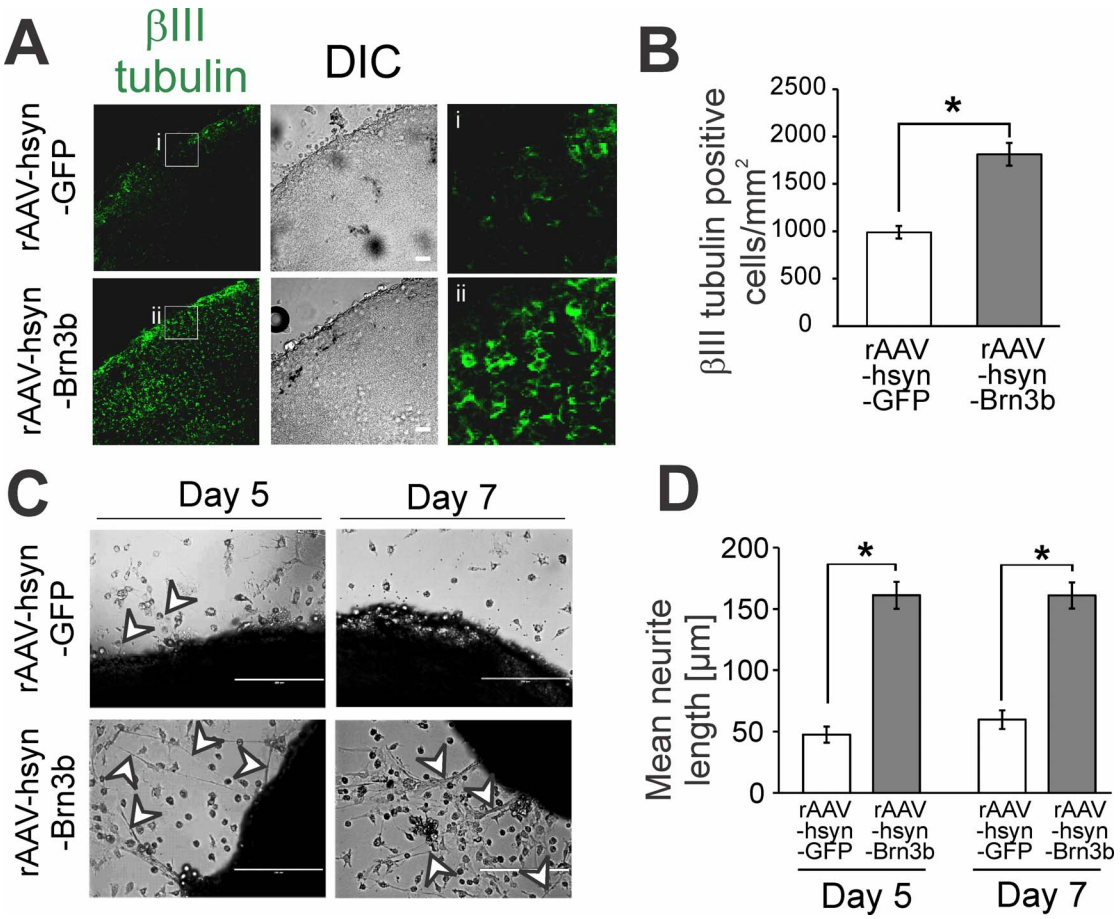

Figure 10. Neuroprotective effects of rAAV-hsyn-Brn3b on RGCs in adult retinal explants. (**A**) Staining for the RGC cell marker β-III-tubulin (*pseudo-green*) on adult rat retinal explants. Immunostaining of RGCs using the RGC specific marker β-III-tubulin confirmed that there was loss of RGCs following 6 days of ex vivo culture after rAAV-hsyn-GFP transduction in comparison to rAAV-hsyn-Brn3b transduced retinal explants. *Insets* (i and ii) represent the magnification of β-III-tubulin–stained images, to show individual cells. (**B**) Attenuation of RGC death was indicated by higher counts of β-III-tubulin–stained cells (characteristic of RGCs) at 6 days ex vivo after rAAV-hsyn-Brn3b (*gray bar*) viral transduction, compared with explants transduced with rAAV-hsyn-GFP virus (*white bar*). Six different explants were assessed from three experiments in each group (*$P < 0.001$ using Mann-Whitney rank sum test). *Scale bar*: 20 μm. (**C**) Phase contrast photomicrographs of retinal explants, grown without trophic factors, transduced either with rAAV-hsyn-GFP or rAAV-hsyn-Brn3b viruses and evaluated 5 and 7 days after explantation. Increased regrowth of neurites (*white arrowheads*) was observed in explants transduced with rAAV-hsyn-Brn3b in comparison with rAAV-hsyn-GFP transduced controls ($n = 7$/group). *Scale bars*: 200 μm. (**D**) Average length of processes emanating from each cultured retinal explant. The average length of neurites in rAAV-hsyn-Brn3b explants was 3.0 ± 0.35 (average ± SEM) times longer than those from rAAV-hsyn-GFP explants. Statistical differences were significant in three independent experiments for rAAV-hsyn-Brn3b explants compared with rAAV-hsyn-GFP explants, (*$P < 0.001$ using Mann-Whitney rank sum test).

maintain microtubule stability and promote neurite outgrowth. In the current study, the increase in ac-Tuba in the posterior region of the optic nerve head and also in the NFL of the retina in IOP-elevated rAAV-CMV-Brn3b–injected rats, could be indicative of the effectiveness of Brn3b in promoting recovery of RGC axons following damage due to IOP.

AbLIM participates in axon outgrowth, guidance, and synaptic trafficking.[53–55] Mutations in abLIM in chick retina have been shown to cause multiple pathfinding errors in RGCs.[6] The resulting abnormalities were strikingly similar to those observed in Brn3b-deficient mice, suggesting that abLIM and Brn3b could be involved together in regulation of pathfinding in RGCs.[6] Our data are consistent with these findings and we detected upregulation of abLIM in rAAV-CMV-Brn3b transduced IOP-elevated rat retinas, which was also observed posterior to the site of axonal injury in the optic nerve head.

Degeneration of axons after injury occurs first in regions of the optic nerve proximal to the laminar region.[56,57] In some animal models of glaucoma, disruption of fast anterograde axonal transport has been shown to result from nerve compression, as a consequence of IOP.[49,58,59] Glaucoma is characterized by a selective dysregulation of axonal transport of membrane-bound organelle, including mitochondria.[49,60] Distal axon injury is predegenerative hallmark in rodent models of glaucoma, which subsequently results in vision loss.[61] The lamina cribrosa in human and lamina-like region in rodents are thought to be the site of axonal transport blockade. There is another school of thought, that axonal transport disruption at the superior colliculus is an earliest hallmark of changes in glaucoma. However, the authors in these studies do not address the site of axonal insult, but focus on the deficits in anterograde transport from the retina.[61,62]

The loss of RGCs and subsequent visual field deficits could be a clear consequence of disruption of axonal transport; however, the underlying mechanisms are not completely understood. In this study, we demonstrate that AAV-derived Brn3b overexpression in IOP-elevated rat eyes is able to reverse

the damage to the optic nerve and restore transport along the axons into the myelinated region of the optic nerve. An immunoblot analysis of CTB in optic nerve extracts would have provided more conclusive evidence, however there are technical limitations of carrying out this experiment. In our experiments we injected 4 μL 0.1% Alexa conjugated cholera toxin B, which would yield less than 1 μg CTB in the total extract from an optic nerve, which is not sufficient for detection by immunoblot analysis.

In addition, AAV-mediated expression of Brn3b protein during ocular hypertension was able to promote increase survival of RGCs, indicative of a neuroprotective role of Brn3b in RGCs. Brn3b overexpression also sustained axonal integrity, which could be due to Brn3b's ability to upregulate GAP-43 as well as other proteins including ac-Tuba, abLIM, and NF-M, which are important for axon stability as well as axonal regeneration.

In vitro explants culture represent an injury model in which axons of RGCs have been severed and is a useful model system to determine the efficacy of different experimental approaches to promote axon outgrowth as well as survival of retinal ganglion cells.[63,64] Our study demonstrated that AAV-mediated expression of Brn3b protein could stimulate neurite outgrowth ex vivo in adult rat RGCs. Increased staining for β-III tubulin in Brn3b transduced rat retinal explants suggests that Brn3b can rescue RGCs from cell death. Apart from being a RGC marker, β-III tubulin also contributes to microtubule stability in neuronal somas and axons by playing an important role in axonal transport and structure.[65] It is also possible that Brn3b could upregulate β-III tubulin in RGCs and this remains to be tested in future studies.

The functional changes in IOP-elevated rat eyes were assessed psychophysiologically using the optomotor response test, which is indicative of subcortical responses to retinal input.[33] As anticipated, our data show that a decline in cycles/degree occurs following IOP elevation in Brown Norway rats. The changes in visual acuity in Morrison's IOP elevation model were not drastic, unlike some rodent optic nerve crush models.[66] These are possibly reflective of the gradual disease process of glaucoma, a slow progressive axonopathy, in which vision loss is detected only after a substantial loss of RGCs has occurred. Brn3b overexpression using the rAAV-hsyn-Brn3b vector was efficacious since it was able to significantly restore the visual acuity that was compromised in IOP-elevated rat eyes. Taken together, the data suggest that targeted AAV-mediated expression of transcription factor Brn3b in RGCs has neuroprotective effects and improves visual function in an animal model of glaucoma.

Acknowledgments

Supported by Department of Defense Grant W81XWH-10-2-0003 (TY [P.I.], RK [Co-I.]), Arlington, Virginia, United States; and in part by National Eye Institute Grant 1R01EY019952 (RK), Bethesda, Maryland, United States.

Disclosure: **D.L. Stankowska**, None; **A.Z. Minton**, None; **M.A. Rutledge**, None; **B.H. Mueller II**, None; **N.R. Phatak**, None; **S. He**, None; **H.-Y. Ma**, None; **M.J. Forster**, None; **T. Yorio**, None; **R.R. Krishnamoorthy**, None

References

1. Quigley HA. Ganglion cell death in glaucoma: pathology recapitulates ontogeny. *Aust N Z J Ophthalmol*. 1995;23:85–91.
2. Gan L, Xiang M, Zhou L, Wagner DS, Klein WH, Nathans J. POU domain factor Brn-3b is required for the development of a large set of retinal ganglion cells. *Proc Natl Acad Sci U S A*. 1996;93:3920–3925.
3. Xiang M. Requirement for Brn-3b in early differentiation of postmitotic retinal ganglion cell precursors. *Dev Biol*. 1998; 197:155–169.
4. Xiang M, Gan L, Li D, et al. Role of the Brn-3 family of POU-domain genes in the development of the auditory/vestibular, somatosensory, and visual systems. *Cold Spring Harb Symp Quant Biol*. 1997;62:325–336.
5. Gan L, Wang SW, Huang Z, Klein WH. POU domain factor Brn-3b is essential for retinal ganglion cell differentiation and survival but not for initial cell fate specification. *Dev Biol*. 1999;210:469–480.
6. Erkman L, Yates PA, McLaughlin T, et al. A POU domain transcription factor-dependent program regulates axon pathfinding in the vertebrate visual system. *Neuron*. 2000;28:779–792.
7. Wang SW, Gan L, Martin SE, Klein WH. Abnormal polarization and axon outgrowth in retinal ganglion cells lacking the POU-domain transcription factor Brn-3b. *Mol Cell Neurosci*. 2000; 16:141–156.
8. Erkman L, McEvilly RJ, Luo L, et al. Role of transcription factors Brn-3.1 and Brn-3.2 in auditory and visual system development. *Nature*. 1996;381:603–606.
9. Husak PJ, Kuo T, Enquist LW. Pseudorabies virus membrane proteins gI and gE facilitate anterograde spread of infection in projection- specific neurons in the rat. *J Virol*. 2000;74:10975–10983.
10. Morrison JC, Moore CG, Deppmeier LM, Gold BG, Meshul CK, Johnson EC. A rat model of chronic pressure-induced optic nerve damage. *Exp Eye Res*. 1997;64:85–96.
11. Zhou Y, Pernet V, Hauswirth WW, Di Polo A. Activation of the extracellular signal-regulated kinase 1/2 pathway by AAV gene transfer protects retinal ganglion cells in glaucoma. *Mol Ther*. 2005;12:402–412.
12. Holländer H, Vaaland JL. A reliable staining method for semithin sections in experimental neurfanatomy. *Brain Res*. 1968; 10:120–126.
13. Chauhan BC, LeVatte TL, Garnier KL, et al. Semiquantitative optic nerve grading scheme for determining axonal loss in experimental optic neuropathy. *Invest Ophthalmol Vis Sci*. 2006;47:634–640.
14. Barres BA, Silverstein BE, Corey DP, Chun LL. Immunological, morphological, and electrophysiological variation among retinal ganglion cells purified by panning. *Neuron*. 1988;1: 791–803.
15. Spencer ML, Theodosiou M, Noonan DJ. NPDC-1, a novel regulator of neuronal proliferation, is degraded by the ubiquitin/proteasome system through a PEST degradation motif. *J Biol Chem*. 2004;279:37069–37078.
16. Park KW, Baik HH, Jin BK. IL-13-induced oxidative stress via microglial NADPH oxidase contributes to death of hippocampal neurons in vivo. *J Immunol*. 2009;183:4666–4674.
17. Shinohara M, Sato N, Kurinami H, et al. Reduction of brain β-amyloid (Aβ) by fluvastatin, a hydroxymethylglutaryl-CoA reductase inhibitor, through increase in degradation of amyloid precursor protein C-terminal fragments (APP-CTFs) and Aβ clearance. *J Biol Chem*. 2010;285:22091–22102.
18. La Marca R, Cerri F, Horiuchi K, et al. TACE (ADAM17) inhibits Schwann cell myelination. *Nat Neurosci*. 2011;14:857–865.
19. Cherry JJ, Osman EY, Evans MC, et al. Enhancement of SMN protein levels in a mouse model of spinal muscular atrophy using novel drug-like compounds. *EMBO Mol Med*. 2013;5: 1035–1050.
20. Frühbeis C, Fröhlich D, Kuo WP, et al. Neurotransmitter-triggered transfer of exosomes mediates oligodendrocyte–neuron communication. *PLoS Biol*. 2013;11:e1001604.

21. Shi Q, Prior M, Zhou X, et al. Preventing formation of reticulon 3 immunoreactive dystrophic neurites improves cognitive function in mice. *J Neurosci*. 2013;33:3059–3066.
22. Grove M, Brophy PJFAK. Is required for Schwann cell spreading on immature basal lamina to coordinate the radial sorting of peripheral axons with myelination. *J Neurosci*. 2014;34:13422–13434.
23. Cui Q, Yip HK, Zhao RCH, So K-F, Harvey AR. Intraocular elevation of cyclic AMP potentiates ciliary neurotrophic factor-induced regeneration of adult rat retinal ganglion cell axons. *Mol Cell Neurosci*. 2003;22:49–61.
24. Morrison JC. Elevated intraocular pressure and optic nerve injury models in the rat. *J Glaucoma*. 2005;14:315–317.
25. Xiang M, Zhou L, Macke JP, et al. The Brn-3 family of POU-domain factors: primary structure, binding specificity, and expression in subsets of retinal ganglion cells and somatosensory neurons. *J Neurosci*. 1995;15(7 pt 1):4762–4785.
26. Le Carré J, Schorderet DF, Cottet S. Altered expression of β-galactosidase-1-like protein 3 (Glb1l3) in the retinal pigment epithelium (RPE)-specific 65-kDa protein knock-out mouse model of Leber's congenital amaurosis. *Mol Vis*. 2011;17:1287–1297.
27. Luo H, Jin K, Xie Z, et al. Forkhead box N4 (Foxn4) activates Dll4-Notch signaling to suppress photoreceptor cell fates of early retinal progenitors. *PNAS*. 2012;109:E553–E562.
28. Chen D, Livne-bar I, Vanderluit JL, Slack RS, Agochiya M, Bremner R. Cell-specific effects of RB or RB/p107 loss on retinal development implicate an intrinsically death-resistant cell-of-origin in retinoblastoma. *Cancer Cell*. 2004;5:539–551.
29. Reed NA, Cai D, Blasius TL, et al. Microtubule acetylation promotes kinesin-1 binding and transport. *Curr Biol*. 2006;16:2166–2172.
30. Dompierre JP, Godin JD, Charrin BC, et al. Histone deacetylase 6 inhibition compensates for the transport deficit in Huntington's disease by increasing tubulin acetylation. *J Neurosci*. 2007;27:3571–3583.
31. Wang H, Minfei W, Chuanjun Z, et al. Neurofilament proteins in axonal regeneration and neurodegenerative diseases. *Neural Regen Res*. 2012;7:620–626.
32. Chauhan BC, Pan J, Archibald ML, LeVatte TL, Kelly MEM, Tremblay F. Effect of intraocular pressure on optic disc topography, electroretinography, and axonal loss in a chronic pressure-induced rat model of optic nerve damage. *Invest Ophthalmol Vis Sci*. 2002;43:2969–2976.
33. Douglas RM, Alam NM, Silver BD, McGill TJ, Tschetter WW, Prusky GT. Independent visual threshold measurements in the two eyes of freely moving rats and mice using a virtual-reality optokinetic system. *Vis Neurosci*. 2005;22:677–684.
34. Baltmr A, Duggan J, Nizari S, Salt TE, Cordeiro MF. Neuroprotection in glaucoma – is there a future role? *Exp Eye Res*. 2010;91:554–566.
35. Ashtari M, Cyckowski LL, Monroe JF, et al. The human visual cortex responds to gene therapy-mediated recovery of retinal function. *J Clin Invest*. 2011;121:2160–2168.
36. Bainbridge JWB, Smith AJ, Barker SS, et al. Effect of gene therapy on visual function in Leber's congenital amaurosis. *N Engl J Med*. 2008;358:2231–2239.
37. Bennett J, Ashtari M, Wellman J, et al. AAV2 gene therapy readministration in three adults with congenital blindness. *Sci Transl Med*. 2012;4:120ra15.
38. Maguire AM, Simonelli F, Pierce EA, et al. Safety and efficacy of gene transfer for Leber's congenital amaurosis. *N Engl J Med*. 2008;358:2240–2248.
39. Minton AZ, Phatak NR, Stankowska DL, et al. Endothelin B receptors contribute to retinal ganglion cell loss in a rat model of glaucoma. *PLoS One*. 2012;7:e43199.
40. Turner EE, Jenne KJ, Rosenfeld MG. Brn-3.2: a Brn-3-related transcription factor with distinctive central nervous system expression and regulation by retinoic acid. *Neuron*. 1994;12:205–218.
41. Naskar R, Thanos S. Retinal gene profiling in a hereditary rodent model of elevated intraocular pressure. *Mol Vis*. 2006;12:1199–1210.
42. Soto I, Oglesby E, Buckingham BP, et al. Retinal ganglion cells downregulate gene expression and lose their axons within the optic nerve head in a mouse glaucoma model. *J Neurosci*. 2008;28:548–561.
43. Weishaupt J, Klöcker N, Bähr M. Axotomy-induced early down-regulation of POU-IV class transcription factors Brn-3a and Brn-3b in retinal ganglion cells. *J Mol Neurosci*. 2005;26:17–26.
44. Biewenga JE, Schrama LH, Gispen WH. Presynaptic phosphoprotein B-50/GAP-43 in neuronal and synaptic plasticity. *Acta Biochim Pol*. 1996;43:327–338.
45. Basi GS, Jacobson RD, Virág I, Schilling J, Skene JHP. Primary structure and transcriptional regulation of GAP-43, a protein associated with nerve growth. *Cell*. 1987;49:785–791.
46. Skene JH, Willard M. Characteristics of growth-associated polypeptides in regenerating toad retinal ganglion cell axons. *J Neurosci*. 1981;1:419–426.
47. Benowitz LI, Apostolides PJ, Perrone-Bizzozero N, Finklestein SP, Zwiers H. Anatomical distribution of the growth-associated protein GAP-43/B-50 in the adult rat brain. *J Neurosci*. 1988;8:339–352.
48. Mu X, Zhao S, Pershad R, et al. Gene expression in the developing mouse retina by EST sequencing and microarray analysis. *Nucleic Acids Res*. 2001;29:4983–4993.
49. Martin KRG, Quigley HA, Valenta D, Kielczewski J, Pease ME. Optic nerve dynein motor protein distribution changes with intraocular pressure elevation in a rat model of glaucoma. *Exp Eye Res*. 2006;83:255–262.
50. Fournier AE, McKerracher L. Tubulin expression and axonal transport in injured and regenerating neurons in the adult mammalian central nervous system. *Biochem Cell Biol*. 1995;73:659–664.
51. Sengottuvel V, Leibinger M, Pfreimer M, Andreadaki A, Fischer D. Taxol facilitates axon regeneration in the mature CNS. *J. Neurosci*. 2011;31:2688–2699.
52. Gaub P, Tedeschi A, Puttagunta R, Nguyen T, Schmandke A, Giovanni SD. HDAC inhibition promotes neuronal outgrowth and counteracts growth cone collapse through CBP/p300 and P/CAF-dependent p53 acetylation. *Cell Death Differ*. 2010;17:1392–1408.
53. Demarco RS, Lundquist EA. RACK-1 acts with Rac GTPase signaling and UNC-115/abLIM in Caenorhabditis elegans axon pathfinding and cell migration. *PLoS Genet*. 2010;6:e1001215.
54. Lundquist EA, Herman RK, Shaw JE, Bargmann CI. UNC-115, a conserved protein with predicted LIM and actin-binding domains, mediates axon guidance in C. elegans. *Neuron*. 1998;21:385–392.
55. Norris AD, Dyer JO, Lundquist EA. The Arp2/3 complex, UNC-115/abLIM, and UNC-34/enabled regulate axon guidance and growth cone filopodia formation in Caenorhabditis elegans. *Neural Dev*. 2009;4:38.
56. Schlamp CL, Li Y, Dietz JA, Janssen KT, Nickells RW. Progressive ganglion cell loss and optic nerve degeneration in DBA/2J mice is variable and asymmetric. *BMC Neurosci*. 2006;7:66.
57. Howell GR, Libby RT, Jakobs TC, et al. Axons of retinal ganglion cells are insulted in the optic nerve early in DBA/2J glaucoma. *J Cell Biol*. 2007;179:1523–1537.
58. Chidlow G, Ebneter A, Wood JPM, Casson RJ. The optic nerve head is the site of axonal transport disruption, axonal cytoskeleton damage and putative axonal regeneration failure

Investigative Ophthalmology & Visual Science

in a rat model of glaucoma. *Acta Neuropathol*. 2011;121:737–751.

59. Salinas-Navarro M, Alarcón-Martínez L, Valiente-Soriano FJ, et al. Ocular hypertension impairs optic nerve axonal transport leading to progressive retinal ganglion cell degeneration. *Exp Eye Res*. 2010;90:168–183.
60. Stokely ME, Brady ST, Yorio T. Effects of endothelin-1 on components of anterograde axonal transport in optic nerve. *Invest Ophthalmol Vis Sci*. 2002;43:3223–3230.
61. Crish SD, Sappington RM, Inman DM, Horner PJ, Calkins DJ. Distal axonopathy with structural persistence in glaucomatous neurodegeneration. *Proc Natl Acad Sci U S A*. 2010;107:5196–5201.
62. Crish SD, Dapper JD, MacNamee SE, et al. Failure of axonal transport induces a spatially coincident increase in astrocyte BDNF prior to synapse loss in a central target. *Neuroscience*. 2013;229:55–70.
63. Lasseck J, Schröer U, Koenig S, Thanos S. Regeneration of retinal ganglion cell axons in organ culture is increased in rats with hereditary buphthalmos. *Exp Eye Res*. 2007;85:90–104.
64. Bull ND, Johnson TV, Welsapar G, DeKorver NW, Tomarev SI, Martin KR. Use of an adult rat retinal explant model for screening of potential retinal ganglion cell neuroprotective therapies. *Invest Ophthalmol Vis Sci*. 2011;52:3309–3320.
65. Niwa S, Takahashi H, Hirokawa N. β-Tubulin mutations that cause severe neuropathies disrupt axonal transport. *EMBO J*. 2013;32:1352–1364.
66. De Lima S, Koriyama Y, Kurimoto T, et al. Full-length axon regeneration in the adult mouse optic nerve and partial recovery of simple visual behaviors. *Proc Natl Acad Sci U S A*. 2012;109:9149–9154.

Investigative Ophthalmology & Visual Science